



Cite this: *RSC Adv.*, 2017, 7, 45856

# Flow synthesis of secondary amines over Ag/Al<sub>2</sub>O<sub>3</sub> catalyst by one-pot reductive amination of aldehydes with nitroarenes†

Ekaterina A. Artiukha,<sup>a</sup> Alexey L. Nuzhdin,<sup>a</sup> Galina A. Bukhtiyarova<sup>a</sup> and Valerii I. Bukhtiyarov<sup>ab</sup>

An alumina-supported silver catalyst was investigated in the one-pot reductive amination of aldehydes with nitroarenes in a continuous flow reactor using molecular hydrogen as a reducing agent. A series of secondary amines containing alkyl, OH, OCH<sub>3</sub>, Cl, Br and C=C groups was synthesized in good to excellent yields. The yield of the secondary amine depends on the rate of formation of an intermediate imine. It was shown that the accumulation of carbonaceous deposits on the catalyst is the main reason of catalyst deactivation. The spent catalyst can be easily regenerated and reused without losing catalytic activity.

Received 14th August 2017  
Accepted 20th September 2017

DOI: 10.1039/c7ra08986d

rsc.li/rsc-advances

## Introduction

Secondary amines are extensively used for production of pharmaceuticals, agrochemicals and fine chemicals.<sup>1</sup> Therefore, developing new highly efficient and environmentally friendly methods for the synthesis of these compounds has received increasing attention lately.<sup>2</sup> One-pot reductive amination of aldehydes with nitroarenes over heterogeneous catalysts using molecular hydrogen or another “green” reducing agent is an atom-economical and environmentally attractive method for synthesis of secondary aromatic amines.<sup>3–6</sup> The process begins with the reduction of the nitroarene to a primary aromatic amine. Further reversible condensation of the primary amine with aldehyde forms the corresponding imine, which is finally reduced to the target secondary amine. In general, the reaction is realized in the presence of noble metal-based catalysts (Pd,<sup>3</sup> Pt,<sup>3k,4a</sup> Ir<sup>4b</sup> and Au<sup>5</sup>). Recently, reductive amination of aldehydes with nitroaromatic compounds has been examined over Fe- and Co-based catalysts comprised of metal particles embedded in mesoporous nitrogen-doped carbon.<sup>6a–f</sup>

Alumina-supported silver catalysts are attractive for reductive amination of aldehydes with nitroarenes due to their activity and high chemoselectivity in hydrogenation of substituted nitroarenes to corresponding anilines.<sup>7a,b</sup> In addition, a series of secondary amines has been synthesized from nitroaromatics and benzyl alcohols over the Ag/Al<sub>2</sub>O<sub>3</sub> catalyst under H<sub>2</sub>.<sup>7c</sup> However, to achieve high yields of desired products this reaction requires the use of KF as a co-catalyst and should

be carried out for a long time over catalyst with high silver loading.

The reductive amination of aldehydes with nitroarenes is routinely performed in batch reactors.<sup>3,4,6</sup> Meanwhile, in recent years the continuous-flow synthesis has emerged as an attractive alternative to batch protocols. Potential benefits of flow chemistry include an enhanced safety profile, superior interfacial mass and energy transfer properties, reduction of the side product formation through a better control over process variables, and shortening of the development time from laboratory to final production levels.<sup>8</sup> Herein, we describe the use of the supported Ag/γ-Al<sub>2</sub>O<sub>3</sub> catalyst for the one-pot reductive amination of aliphatic and aromatic aldehydes with nitroarenes in a continuous flow reactor.

## Experimental

### Chemicals

Silver nitrate (99.5%), nitrobenzene (99%), *o*-nitrotoluene (99+%), *m*-nitrotoluene (99%), *p*-nitrotoluene (99%), *p*-nitrophenol (99%), *p*-chloronitrobenzene (99%), *p*-bromonitrobenzene (99%), *n*-heptanal (95%), 3-phenylpropionaldehyde (95%), undecylenic aldehyde (97%), 3-methylcrotonaldehyde (97%), benzaldehyde (98+%), *p*-anisaldehyde (99+%), *p*-chlorobenzaldehyde (98.5+%), 2-heptanone (98%), *n*-decane (99+%) from Acros Organics, as well as *p*-ethylnitrobenzene (95%) from Sigma-Aldrich, were used without additional purification. Toluene of 99.5% purity from ECOS (Russia) was employed as a solvent.

### Catalyst preparation

The γ-Al<sub>2</sub>O<sub>3</sub> support was prepared by extrusion of a paste obtained by mixing of aluminum oxide (Puralox TH 100/150,

<sup>a</sup>Boreskov Institute of Catalysis SB RAS, Novosibirsk, 630090, Russia. E-mail: anuzhdin@catalysis.ru

<sup>b</sup>Novosibirsk State University, Novosibirsk, 630090, Russia

† Electronic supplementary information (ESI) available. See DOI: 10.1039/c7ra08986d



Sasol), aluminum hydroxide (Disperal, Sasol) and aqueous solution of nitric acid.<sup>5c</sup> An Ag/Al<sub>2</sub>O<sub>3</sub> catalyst was prepared by impregnating of  $\gamma$ -Al<sub>2</sub>O<sub>3</sub> (grain size of 250–500  $\mu$ m) with an aqueous solution of silver nitrate followed by drying at 70 °C under vacuum and calcination in air at 500 °C for 3 h.<sup>7a</sup>

### Catalyst characterization

The Ag content was measured by XRF using an ARL instrument. Textural characteristics were determined from nitrogen adsorption–desorption isotherms (77 K) obtained on a Micromeritics ASAP 2400 analyzer. Powder XRD patterns were recorded on a Bruker D8 diffractometer using CuK $\alpha$  radiation and a LynxEye position sensitive detector. X-ray photoelectron spectra (XPS) were obtained on a SPECS (Germany) spectrometer equipped with a PHOIBOS-150 hemispherical energy analyzer and the X-ray source with double Al/Mg anode. TEM studies were performed with a JEM-2010 electron microscope (JEOL, Japan). TG-DSC-MS measurement was conducted using an apparatus consisting of a STA 449 F1 Jupiter thermal analyzer and a QMS 403D Aëolos quadrupole mass spectrometer (NETZSCH, Germany) as described earlier.<sup>5c</sup>

### Reductive amination of aldehydes with nitroarenes

The catalytic properties were investigated under continuous-flow conditions in H-Cube Pro™ setup (Thalesnano, Hungary) equipped with packed-bed reactors CatCart® 30 (length of 30 mm, inner diameter of 4 mm).<sup>5c</sup> Before each catalytic run, the catalyst (0.215 g) was reduced by a mixture of hydrogen with toluene at 110 °C and 3.0 MPa for 1 hour (flow rates of toluene and H<sub>2</sub>: 0.5 and 60 mL min<sup>-1</sup>, respectively). The inlet was then switched to the flask with the solution of nitroarene (0.025 M) and aldehyde (0.0375 M) in toluene. This moment was chosen as the starting point of the reaction. The catalytic tests were carried out at 100–110 °C, 3.0 MPa of hydrogen pressure, liquid and hydrogen feed rates of 0.5 and 60 mL min<sup>-1</sup>, respectively. As a result of special tests, we found earlier that there is no influence of external or internal mass transfer limitations under the conditions used.<sup>9</sup> The performance of the catalyst was evaluated by analysis of the samples taken 30–34 min after the beginning of the experiment. The reaction products were analyzed by GC (Agilent 6890N instrument with a HP 5-MS capillary column 60 m  $\times$  320  $\mu$ m  $\times$  0.25  $\mu$ m) using *n*-decane as the internal standard. The product yields were calculated based

on nitro compounds. The reaction products were identified by GC-MS (Agilent 7000B Triple Quad System) and comparing the GC retention times with the authentic compounds.<sup>5b,c</sup>

## Results and discussion

The Ag/Al<sub>2</sub>O<sub>3</sub> catalyst was prepared by incipient wetness impregnation of the  $\gamma$ -Al<sub>2</sub>O<sub>3</sub> support with an aqueous solution of silver nitrate.<sup>7a,10a</sup> The physico-chemical characteristics of the

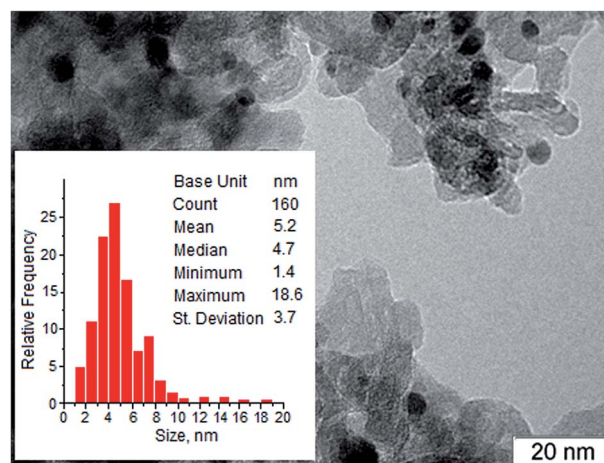


Fig. 1 TEM data of the as-prepared Ag/Al<sub>2</sub>O<sub>3</sub> catalyst.

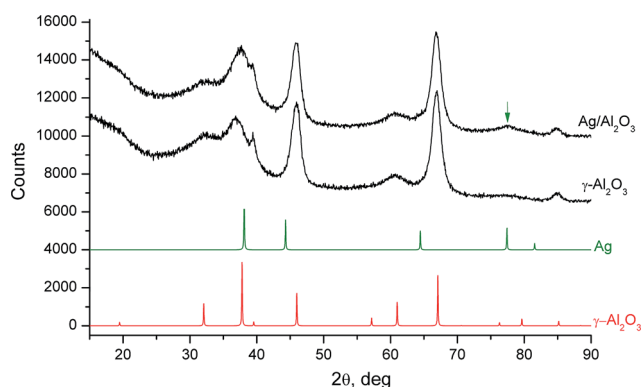


Fig. 2 Powder XRD patterns of the Ag/Al<sub>2</sub>O<sub>3</sub> catalyst and  $\gamma$ -Al<sub>2</sub>O<sub>3</sub> support.

Table 1 Physico-chemical characteristics of the as-prepared, spent and regenerated Ag/Al<sub>2</sub>O<sub>3</sub> catalyst

	As-prepared	Spent <sup>a</sup>	Regenerated
Content of Ag, wt%	4.7	4.7	4.6
Mean particle size, nm	5.2	5.1	5.3
BET surface area, m <sup>2</sup> g <sup>-1</sup>	175 <sup>b</sup> , 167	140	147
Total pore volume, cm <sup>3</sup> g <sup>-1</sup>	0.63 <sup>b</sup> , 0.61	0.53	0.55
Mean pore diameter, nm	15.0 <sup>b</sup> , 14.7	14.9	14.9
Content of carbonaceous deposits, wt%	—	4.2	≈ 0

<sup>a</sup> After 2.5 h on-stream at 100 °C, *p*(H<sub>2</sub>) = 3.0 MPa, nitrobenzene (0.025 M), *n*-heptanal (0.0375 M). <sup>b</sup>  $\gamma$ -Al<sub>2</sub>O<sub>3</sub> support.



Table 2 Reductive amination of aldehydes with nitroarenes over Ag/Al<sub>2</sub>O<sub>3</sub> catalyst<sup>a</sup>

Entry	1	2	T, °C	Conversion of 1	Conversion of 2	Yield <sup>b</sup> , %			
						3	4	5	Others
1			100	>99	70	15	6	79	n.d. <sup>c</sup>
2 <sup>d</sup>			100	>99	61	22	11	67	n.d.
3			100	>99	72	44	15	41	n.d.
4			100	>99	76	11	4	85	n.d.
5			100	>99	80	5	5	90	n.d.
6			110	>99	88	5	3	92	n.d.
7			100	>99	78	6	5	89	n.d.
8			100	>99	71	4	6	84	6 <sup>e</sup>
9			100	89	56	13	6	70	n.d.
10			110	>99	65	15	6	79	n.d.
11			100	92	59	12	7	73	n.d.
12			110	>99	64	14	5	81	n.d.
13			110	>99	89	6	2	92	n.d.
14			110	>99	81	11	11	78	n.d.
15			110	>99	87	16	n.d.	82	2
16			110	>99	97	17	4	79	n.d.
17			100	>99	94	4	9	86	1
18			100	>99	95	3	n.d.	87	1 + 9 <sup>e</sup>



Table 2 (Contd.)

Entry	1	2	T, °C	Conversion of 1	Conversion of 2	Yield <sup>b</sup> , %			
						3	4	5	Others
19			110	>99	69	13	6	81	n.d.
20			100	>99	74	6	9	85	n.d.

<sup>a</sup> 1 (0.025 M), 2 (0.0375 M), Ag/Al<sub>2</sub>O<sub>3</sub> catalyst = 215 mg, toluene, *p*(H<sub>2</sub>) = 3.0 MPa, reaction time = 30–34 min, liquid and hydrogen feed rates of 0.5 and 60 mL min<sup>-1</sup>, respectively. <sup>b</sup> The product yields were calculated based on nitro compounds by using GC. <sup>c</sup> n.d. = not detected. <sup>d</sup> No pre-reduction treatment was conducted. <sup>e</sup> Tertiary amine.

catalyst are summarized in Table 1. Fig. 1 shows a TEM image of the Ag/Al<sub>2</sub>O<sub>3</sub> catalyst, the pattern is typical of the metallic Ag nanoparticles supported on alumina.<sup>7a,10a,b</sup> The nanoparticles distributed well on the support were mainly between 1 and 10 nm in size, with the mean particle size about 5 nm. Powder XRD patterns of the pre-reduced Ag/Al<sub>2</sub>O<sub>3</sub> catalyst and  $\gamma$ -Al<sub>2</sub>O<sub>3</sub> support are shown in Fig. 2. The XRD pattern of the Ag/Al<sub>2</sub>O<sub>3</sub> catalyst contains peaks associated with  $\gamma$ -Al<sub>2</sub>O<sub>3</sub>, while the most intensive signal of metallic silver at  $2\theta = 38.07^\circ$  is overlapped with the signal of alumina and is not clearly observed because of small sizes of silver nanoparticles. Nevertheless, the low-intensity broad diffraction peak at  $2\theta = 77.46^\circ$  is seen on the diffraction curve that could be attributed to the (311) plane of the metallic silver phase.

The Ag 3d XPS and Ag MVV Auger spectra of the as-prepared and pre-reduced Ag/Al<sub>2</sub>O<sub>3</sub> catalysts (ESI<sup>†</sup>) were measured to identify the silver chemical state on the catalyst surfaces. According to the XPS data, both Ag/Al<sub>2</sub>O<sub>3</sub> catalysts contain silver in the oxidized state. We suppose that the oxidation of silver particles, even in the pre-reduced catalysts, occurs *via* contact with atmospheric oxygen during the transfer of the sample from catalytic reactor to the spectrometer. The ability of the supported silver nanoparticles to react with oxygen at ambient conditions is confirmed by the observation that color of the catalysts changes immediately upon its retrieval from the reactor after reduction or catalytic experiments. Therefore, the Ag/Al<sub>2</sub>O<sub>3</sub> catalyst should be pre-reduced directly before reaction. Indeed, the preliminary experiments show the appreciable increase in the yields of secondary amines over the Ag/Al<sub>2</sub>O<sub>3</sub> catalyst after pre-reduction (Table 2, entries 1 and 2).

The Ag/Al<sub>2</sub>O<sub>3</sub> catalyst has been studied in the one-pot reductive amination of aldehydes with nitroarenes in a continuous flow reactor using toluene as a solvent (Table 2). Since aldehyde could produce the corresponding alcohol in a side

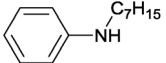
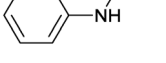
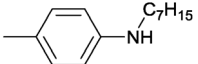
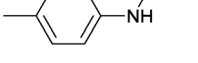
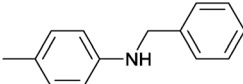
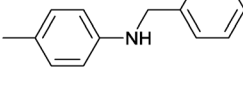
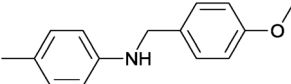
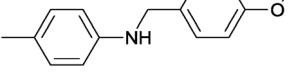
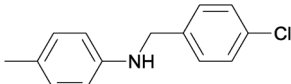
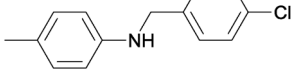
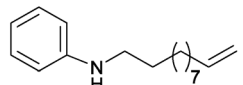
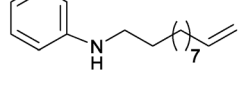
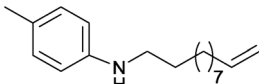
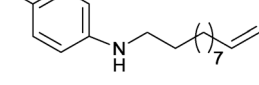
reaction<sup>5b,c</sup> the reaction was carried out at a 1.5-fold excess of aldehyde. It was found that various secondary amines could be obtained over the Ag/Al<sub>2</sub>O<sub>3</sub> catalyst in yield up to 92% (Table 2). The introduction of electron-donating substituents (CH<sub>3</sub>, CH<sub>2</sub>CH<sub>3</sub> and OH) in the *para*- and *meta*-positions of nitrobenzene improved the yield of secondary amines (Table 2, entries 1 and 4–8). At the same time, in the case of nitroarenes with electron-withdrawing substituents (Cl, Br) in the *para*-position or methyl substituent in the *ortho*-position a reduction in the yield of the target products was observed under the same reaction conditions (Table 2, entries 3, 9 and 11). The observed effect of substituents can be explained by their impact on the nucleophilic properties of intermediate primary aromatic amines. So, anilines with electron-donating substituents in the *meta*- and *para*-positions have stronger nucleophilic properties that lead to an increase in the imine formation rate through the reaction with aldehyde.<sup>5c</sup> It should be noted that no conversion of aldehydes or nitroarenes was observed over pure  $\gamma$ -alumina under the reaction conditions.

Aliphatic aldehydes (*n*-heptanal and 3-phenylpropionaldehyde) gave higher yields of secondary amine in reaction with *p*-nitrotoluene than benzaldehyde derivatives (Table 2, entries 6 and 13–16). It can be explained by faster interaction between *p*-toluidine formed during the reaction and aliphatic aldehydes due to stronger electrophilic properties of the latter.<sup>5b</sup> The utilization of 2-heptanone instead of aldehydes led to formation of secondary amines in negligible yield, which is connected with much weaker electrophilic properties of ketones. Thus, the yield of secondary amine is determined by the rate of imine formation.

The Ag/Al<sub>2</sub>O<sub>3</sub> catalyst was also investigated in the reductive amination of unsaturated aliphatic aldehydes such as 3-methylcrotonaldehyde and undecylenic aldehyde with nitroarenes. Interestingly, the hydrogenation of carbon–carbon double bond



Table 3 Space time yield (STY) of the secondary amines for the Ag/Al<sub>2</sub>O<sub>3</sub> and Au/Al<sub>2</sub>O<sub>3</sub> catalysts<sup>a</sup>

Entry	Catalyst	Product	<i>T</i> , °C	<i>p</i> , MPa	STY, g(product) g(metal) <sup>-1</sup> h <sup>-1</sup>	Reference
1	4.7% Ag/Al <sub>2</sub> O <sub>3</sub>		100	3	11.2	This work
2	2.5% Au/Al <sub>2</sub> O <sub>3</sub>		80	5	26.9	5b
3	4.7% Ag/Al <sub>2</sub> O <sub>3</sub>		110	3	14.0	This work
4	2.5% Au/Al <sub>2</sub> O <sub>3</sub>		80	5	30.4	5b
5	4.7% Ag/Al <sub>2</sub> O <sub>3</sub>		110	3	11.4	This work
6	2.5% Au/Al <sub>2</sub> O <sub>3</sub>		80	5	26.9	5b
7	4.7% Ag/Al <sub>2</sub> O <sub>3</sub>		110	3	13.8	This work
8	2.5% Au/Al <sub>2</sub> O <sub>3</sub>		80	5	26.2	5b
9	4.7% Ag/Al <sub>2</sub> O <sub>3</sub>		110	3	13.6	This work
10	2.5% Au/Al <sub>2</sub> O <sub>3</sub>		90	5	29.2	5b
11	4.7% Ag/Al <sub>2</sub> O <sub>3</sub>		110	3	14.7	This work
12	2.5% Au/Al <sub>2</sub> O <sub>3</sub>		90	5	31.2	5c
13	4.7% Ag/Al <sub>2</sub> O <sub>3</sub>		100	3	16.3	This work
14	2.5% Au/Al <sub>2</sub> O <sub>3</sub>		90	5	36.9	5c

<sup>a</sup> Nitroarene (0.025 M), aldehyde (0.0375 M), toluene, liquid and hydrogen feed rates of 0.5 and 60 mL min<sup>-1</sup>, respectively.

is almost absent in the reactions of nitrobenzene and *p*-nitrotoluene with unsaturated aliphatic aldehydes (Table 2, entries 17–20). In this case, the unsaturated secondary amines have been obtained as the main products in yield of 81–87%. Moreover, it should be noted that Cl and Br groups have remained unconverted during the reaction (Table 2, entries 9–12 and 16) while the partial hydrogenation of OCH<sub>3</sub> group has been observed (Table 2, entry 15).

In our previous works the 2.5% Au/Al<sub>2</sub>O<sub>3</sub> catalyst with the mean gold particle diameter equal to 3.4 nm was proposed for one-pot reductive amination of aldehydes with nitroarenes in a flow reactor.<sup>5b,c</sup> The targeted secondary amines were obtained in yield up to 99% at 80–100 °C and 5.0 MPa of hydrogen pressure. To compare the catalytic performance of silver and gold catalysts the space time yield (STY) were calculated for the 4.7% Ag/Al<sub>2</sub>O<sub>3</sub> and 2.5% Au/Al<sub>2</sub>O<sub>3</sub> catalysts. The STY is defined as the mass of the secondary amine (g) produced during 1 h per mass of metal (g) in the catalyst.<sup>11</sup> As shown in Table 3, STY of secondary amines for the Ag/Al<sub>2</sub>O<sub>3</sub> catalyst was 1.9–2.4 times lower than that for the Au/Al<sub>2</sub>O<sub>3</sub> catalyst. However, gold is more than 70 times more expensive than silver.<sup>12</sup>

The time-on-stream performance of the Ag/Al<sub>2</sub>O<sub>3</sub> catalyst in reductive amination of *n*-heptanal with nitrobenzene showed a decrease in the secondary amine yield (Fig. 3). To assess the impact of various factors on the catalyst deactivation the as-prepared and spent Ag/Al<sub>2</sub>O<sub>3</sub> catalysts were investigated using XRF, low-temperature nitrogen adsorption, TEM and TG-DSC-

MS analysis. It was found that Ag content, textural properties and silver particle size did not change visibly after reaction (Table 1). Simultaneously, TG-DSC-MS analysis indicated that the spent catalyst contained approximately 4.2 wt% of hydrogen-enriched carbonaceous species (ESI<sup>†</sup>). Therefore, the catalyst deactivation can be explained by the formation of carbonaceous deposits on the catalyst surface.<sup>5b,c,13</sup>

The activity of the spent Ag/Al<sub>2</sub>O<sub>3</sub> catalyst can be restored completely after the oxidative treatment in air at 330 °C for 20 h

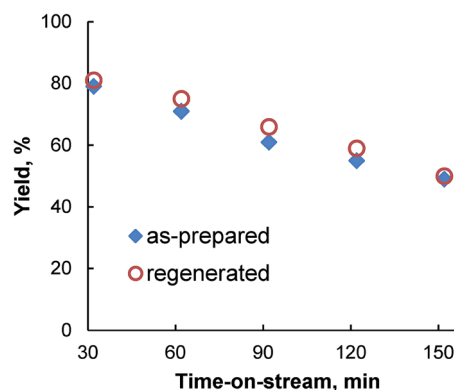


Fig. 3 The time dependence of secondary amine yield in the reaction between nitrobenzene (0.025 M) and *n*-heptanal (0.0375 M) over the as-prepared and regenerated Ag/Al<sub>2</sub>O<sub>3</sub> catalysts at 100 °C and *p*(H<sub>2</sub>) = 3.0 MPa.



(Fig. 3).<sup>5c</sup> This procedure leads to almost complete removal of carbonaceous deposits accumulated on the catalyst without deterioration of textural structure (Table 1) and aggregation of the silver nanoparticles (ESI†).

## Conclusion

The Ag/ $\gamma$ -Al<sub>2</sub>O<sub>3</sub> catalyst is efficient for one-pot reductive amination of aliphatic and aromatic aldehydes with nitroarenes under continuous-flow conditions. Various secondary aromatic amines containing alkyl, OH, OCH<sub>3</sub>, Cl, Br and C=C groups were obtained in good to excellent yields using molecular hydrogen as a reducing agent. The yield of secondary amine is determined by the rate of imine formation. It was shown that the accumulation of carbonaceous deposits on the catalyst is the main reason of catalyst deactivation. The activity of the spent catalyst can be restored completely after the oxidative treatment in air.

## Conflicts of interest

There are no conflicts to declare.

## Acknowledgements

The authors thank A. V. Ishchenko, E. A. Derevyannikova, Dr A. V. Bukhtiyarov and I. A. Zharkova for their help in carrying out this study. This work was conducted within the framework of budget project No. 0303-2016-0006 for Boreskov Institute of Catalysis.

## References

- 1 R. N. Salvatore, C. H. Yoon and K. W. Jung, *Tetrahedron*, 2001, **57**, 7785.
- 2 (a) M. J. Climent, A. Corma and S. Iborra, *Chem. Rev.*, 2011, **111**, 1072; (b) K. Shimizu, *Catal. Sci. Technol.*, 2015, **5**, 1412.
- 3 (a) M. O. Sydnes, M. Kuse and M. Isobe, *Tetrahedron*, 2008, **64**, 6406; (b) B. Sreedhar, P. S. Reddy and D. K. Devi, *J. Org. Chem.*, 2009, **74**, 8806; (c) M. M. Dell'Anna, P. Mastroilli, A. Rizzuti and C. Leonelli, *Appl. Catal., A*, 2011, **401**, 134; (d) M. O. Sydnes and M. Isobe, *Tetrahedron Lett.*, 2008, **49**, 1199; (e) J. Zhou, Z. Dong, P. Wang, Z. Shi, X. Zhou and R. Li, *J. Mol. Catal. A: Chem.*, 2014, **382**, 15; (f) S. Wei, Z. Dong, Z. Ma, J. Sun and J. Ma, *Catal. Commun.*, 2013, **30**, 40; (g) L. Li, Z. Niu, S. Cai, Y. Zhi, H. Li, H. Rong, L. Liu, L. Liu, W. He and Y. Li, *Chem. Commun.*, 2013, **49**, 6843; (h) M. Nasrollahzadeh, *New J. Chem.*, 2014, **38**, 5544; (i) H. Li, Z. P. Dong, P. Wang, F. Zhang and J. Ma, *React. Kinet., Mech. Catal.*, 2013, **108**, 107; (j) P. Wang, H. Liu, J. Niu, R. Li and J. Ma, *Catal. Sci. Technol.*, 2014, **4**, 1333;
- (k) F. G. Cirujano, A. Leyva-Perez, A. Corma and F. X. Llabres i Xamena, *ChemCatChem*, 2013, **5**, 538.
- 4 (a) L. Hu, X. Cao, D. Ge, H. Hong, Z. Guo, L. Chen, X. Sun, J. Tang, J. Zheng, J. Lu and H. Gu, *Chem.–Eur. J.*, 2011, **17**, 14283; (b) M. Pintado-Sierra, A. M. Rasero-Almansa, A. Corma, M. Iglesias and F. Sanchez, *J. Catal.*, 2013, **299**, 137.
- 5 (a) Y. Yamane, X. Liu, A. Hamasaki, T. Ishida, M. Haruta, T. Yokoyama and M. Tokunaga, *Org. Lett.*, 2009, **11**, 5162; (b) E. A. Artiukha, A. L. Nuzhdin, G. A. Bukhtiyarova, S. Yu. Zaytsev, P. E. Plyusnin, Yu. V. Shubin and V. I. Bukhtiyarov, *Catal. Sci. Technol.*, 2015, **5**, 4741; (c) A. L. Nuzhdin, E. A. Artiukha, G. A. Bukhtiyarova, S. Yu. Zaytsev, P. E. Plyusnin, Yu. V. Shubin and V. I. Bukhtiyarov, *RSC Adv.*, 2016, **6**, 88366; (d) Q. Zhang, S.-S. Li, M.-M. Zhu, Y.-M. Liu, H.-Y. He and Y. Cao, *Green Chem.*, 2016, **18**, 2507.
- 6 (a) T. Stemmler, A.-E. Surkus, M.-M. Pohl, K. Junge and M. Beller, *ChemSusChem*, 2014, **7**, 3012; (b) T. Stemmler, F. A. Westerhaus, A.-E. Surkus, M.-M. Pohl, K. Junge and M. Beller, *Green Chem.*, 2014, **16**, 4535; (c) X. Cui, K. Liang, M. Tian, Y. Zhu, J. Ma and Z. Dong, *J. Colloid Interface Sci.*, 2017, **501**, 231; (d) P. Zhou, Z. Zhang, L. Jiang, C. Yu, K. Lv, J. Sun and S. Wang, *Appl. Catal., B*, 2017, **210**, 522; (e) P. Zhou and Z. Zhang, *ChemSusChem*, 2017, **10**, 1892; (f) P. Zhou, C. Yu, L. Jiang, K. Lv and Z. Zhang, *J. Catal.*, 2017, **352**, 264.
- 7 (a) K. Shimizu, Y. Miyamoto and A. Satsuma, *J. Catal.*, 2010, **270**, 86; (b) C. Paun, G. Słowik, E. Lewin and J. Sa, *RSC Adv.*, 2016, **6**, 87564; (c) K. Shimizu, K. Shimura, M. Nishimura and A. Satsuma, *ChemCatChem*, 2011, **3**, 1755.
- 8 (a) C. Wiles and P. Watts, *Green Chem.*, 2014, **16**, 55; (b) M. Irfan, T. N. Glasnov and C. O. Kappe, *ChemSusChem*, 2011, **4**, 300; (c) N. G. Anderson, *Org. Process Res. Dev.*, 2012, **16**, 852; (d) I. R. Baxendale, L. Brocken and C. J. Mallia, *Green Process. Synth.*, 2013, **2**, 211.
- 9 A. L. Nuzhdin, B. L. Moroz, G. A. Bukhtiyarova, S. I. Reshetnikov, P. A. Pyrjaev, P. V. Aleksandrov and V. I. Bukhtiyarov, *ChemPlusChem*, 2015, **80**, 1741.
- 10 (a) R. Poreddy, E. J. García-Suárez, A. Riisager and S. Kegnaes, *Dalton Trans.*, 2014, **43**, 4255; (b) H. Kannisto, K. Arve, T. Pingel, A. Hellman, H. Harelind, K. Eranen, E. Olsson, M. Skoglundh and D. Yu. Murzin, *Catal. Sci. Technol.*, 2013, **3**, 644.
- 11 Y. Aouat, G. Marom, D. Avnir, V. Gelman, G. E. Shter and G. S. Grader, *J. Phys. Chem. C*, 2013, **117**, 22325.
- 12 <http://goldprice.org/gold-silver-ratio.html>.
- 13 A. L. Nuzhdin, S. I. Reshetnikov, G. A. Bukhtiyarova, B. L. Moroz, E. Yu. Gerasimov, P. A. Pyrjaev and V. I. Bukhtiyarov, *Catal. Lett.*, 2017, **147**, 572.

